J. Phys. Chem. C **2009,** *113,* 5947–5951

Perpendicular Superlattice Growth of Hydrophobic Gold Nanorods on Patterned Silicon Substrates via Evaporation-Induced Self-Assembling

Xiaoming Zhang and Toyoko Imae*

Graduate School of Science and Technology, Keio University, Hiyoshi, Yokohama 223-8522, Japan

Received: October 7, 2008; Revised Manuscript Received: February 1, 2009

A simple and efficient route has been reported for the perpendicular superlattice self-assembling of hydrophobic gold nanorods (NRs) based on solvent evaporation. The combination of top-down surface patterning and bottom-up material assembling was used for area-selective gold NR superlattices. The superlattice preferably deposited with a perpendicular orientation of gold NRs on the hydrophobic stripe region in the patterned substrate. The superlattice occupied broad areas up to several square millimeters and possessed an uppermost surface of hexagonally close-packed NR monolayers.

Introduction

Assemblies of metal/semiconductor nanorods (NRs) are attractive research targets due to their unique properties originating with periodic structures at the nanoscale. Gold NRs are particularly suitable for photonic, optoelectronic, and biotechnological applications in the near-infrared spectral region. However, the fabrication of an ordered self-assembly of anisotropic NRs is a great challenge because both positional and orientational alignments on a large scale are required for the application as devices in industry. Various efforts have been made to design suitable techniques to organize NRs, such as template methods based on thermal evaporation and electrodeposition;[1,2] evaporation methods driven by external forces, for example, electric or magnetic field;[3,4] and Langmuir−Blodgett methods at air−liquid interfaces.[5]

Although the deposition through evaporation of solvent without external forces is easy and economical, NR superlattices with an axial alignment perpendicular to the substrate through self-assembling are not prepared in a controlled manner using this method.[6−10] Therefore, techniques combining self-assembling with chemical or topological patterning of the substrate are well-suited to address this limitation.[11−16] However, such significant challenges with reproducibility and uniformity are still in the category of the NR aggregates. Although tackling theses challenges has turned to the controlled assembling and significant progress has been made,[17,18] in NR assembling, there still remain unresolved obstacles, for example, positional and orientational alignment, especially for perpendicular ordering in order to specify the photonic and optoelectronic properties. To our knowledge, up to now, research is scarcely available on the fabrication of NR's ordered self-assembly by the combination of top-down surface patterning and bottom-up material assembling.

Large-scale ordered structures consisting of nanocrystals, especially anisotropic NRs, can have unique properties toward a broad range of applications, and many investigations on nanocrystal self-assembly have been reported.[3−9,19] As an example of large-area arrays with a perpendicular and close-packed alignment, highly monodisperse CdSe/CdS core−shell NRs synthesized by the seeded-growth approach have been found to form vertical superlattices of ca. 1 μm^2 area.[19] The surface interaction-based method was also applied to vertical assembling (ca. 2 μm^2) of aligned CdS NRs on highly oriented pyrolytic graphite.[8] However, in both papers mentioned above, an additional external electric field was applied during the solvent evaporation from a NR-containing solution.

In the present paper, a silicon substrate with topological patterning is adopted and a simple strategy for assembling the highly ordered and aligned NR arrays on such a silicon substrate is presented based on evaporation-induced self-assembling. Importantly, this approach to the assembly does not require any external electric or magnetic fields. Moreover, the size of NR superlattices can enlarge up to several square millimeters.

Experimental Section

Materials. All chemicals were commercially available and used without further purification. Ultrapure water (>18.2 MΩ) was used throughout all the experiments. Hydrophobic gold NRs were synthesized according to a previously published method.[9]

Preparation of *n*-Octadecyltrimethoxysilane (ODS) Self-Assembled Monolayer (SAM) on a Silicon Substrate. The ODS-SAM was fabricated on a piranha-cleaned n-type silicon (100) substrate (NILACO, Japan, resistivity 0.02 Ω·cm) through a vapor-phase method.[20,21] A silicon plate (cleaned with a piranha solution) was placed together with a glass cup filled with ODS liquid in a Teflon container. The container was sealed and placed in an oven maintained at 150 °C for 3 h. After that, the silicon substrate was used without any further treatment.

Preparation of ODS-SAM Pattern on a Silicon Substrate. The fabrication process was performed as follows: First, a silicon wafer was dried with N_2 gas, and then, a solution of positive photoresist (poly(methyl methacrylate), PMMA, OEBR-1000LB 220 cP, Tokyo Ohka Co., Ltd.) was spin-coated at 6000 rpm for 60 s. After heating at 170 °C for 30 min in a convection oven, the line-masked specimen was exposed for 1 min under vacuum ultraviolet light generated from an excimer lamp (Ushio Electric, UER20−172V, $\lambda = 172$ nm, with a power density of 10 mW/cm^2) under the presence of atmospheric oxygen molecules at a pressure of 1.4×10^2 Pa. This step was followed by developing the solvent (methyl isobutyl ketone/isopropyl alcohol = 1:1 (v/v)) to remove the exposed photoresist. The silicon substrate was then etched using a 20% (w/w) KOH solution for 5 s at 60−70 °C. The depth of the patterns was

---

* Corresponding author. Phone: +81-45-566-1799. E-mail: imae@nano.chem.nagoya-u.ac.jp, imae@mail.ntust.edu.tw.

10.1021/jp808864v CCC: $40.75

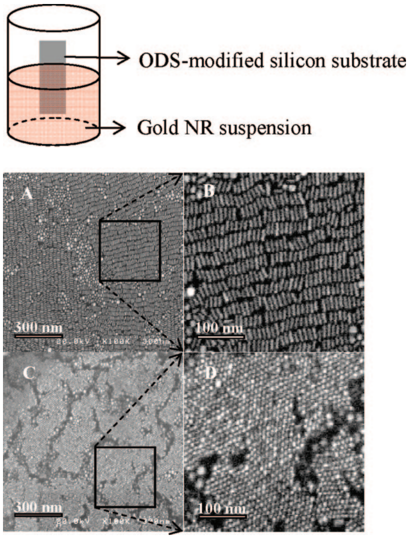

Figure 1. SEM images of a gold NR monolayer with a parallel (A) and perpendicular (C) orientation on an ODS-modified silicon substrate. (B) and (D) are the magnified images of the square region in (A) and (C), respectively. The experimental cell is also illustrated. UV−vis absorbance at a longitudinal band of NR dispersion is 0.3.

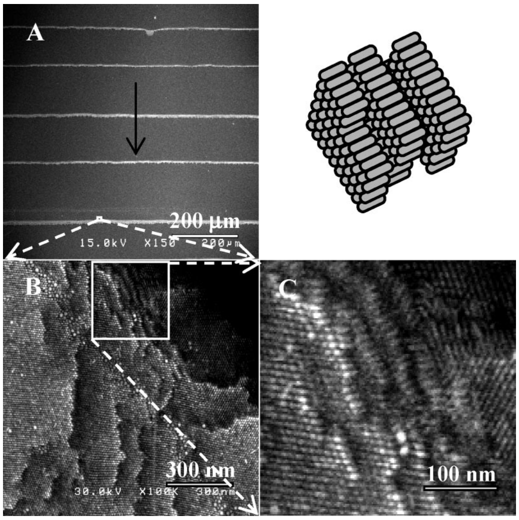

Figure 2. (A) SEM image of spontaneous striped pattern on an ODS-modified silicon substrate, (B) multilayer perpendicular array of gold NRs in a stripe, and (C) magnified image of square region in (B). A gold NR array is also illustrated. The arrow in (A) indicates the downtrend of the liquid interface. UV−vis absorbance at longitudinal band of NR dispersion is 1.4.

about 20−30 nm. After that, ODS-SAMs were obtained by gas-phase evaporation of ODS. Finally, after the photoresist was removed by acetone, the specimen was rinsed with water and then dried with N_2 gas. The specimen was used without further treatment.

Superlattice Growth of Gold NRs on Silicon Substrates. In a typical experiment, a piece of silicon plate was immersed vertically into a $CHCl_3$ solution of gold NRs, which was kept stationary in a glass bottle at room temperature (23 ± 1 °C). $CHCl_3$ was then allowed to gradually evaporate (at the evaporation rate of 1 mm/h) in air. This procedure must be carried out carefully because the evaporation rate is the important control parameter. During this period, the substrate should be kept free from touching the wall of the bottle.

Preparation of Self-Assembled NR Films on a Copper Grid. TEM samples were prepared by developing a $CHCl_3$ suspension of NRs onto the surface of water, evaporating the solvent thoroughly, and transferring part of the floating films on collodion/carbon-coated Cu grids (100 mesh, 3 mm).

Measurements. Scanning electron microscopy (SEM, Hitachi, S-4500), transmission electron microscopy (TEM, Philips, TECNAI SPIRIT), and high-resolution TEM (Philips, TECNAI F20) were employed.

Results and Discussion

Growth of Gold NR Superlattices at a Low NR Concentration on a Homogeneous ODS-SAM Substrate. In this paper, gold NRs with lengths of 20−25 nm and diameters of 5−6 nm were used (the aspect ratio was about 3.5; see Figure S1 in the Supporting Information). The assembly of anisotropic NRs was prepared by gradual evaporation of solvent, as described in the Experimental Section. An experimental cell is illustrated in Figure 1. One of the merits of this method is that most impurities, such as side products of the ODS hydrolysis and larger gold particles, will remain in the suspension as the evaporation progresses. Thus, such impurities do not disturb the assembling. Another merit is that the evaporation process is carried out at a steady speed, as long as the external conditions, such as temperature and humidity are kept invariant during the specimen preparation period. In addition, the concentration change of the NR suspension can be less. The reason is that large numbers of NRs deposit on the interior wall of the glass bottle at the same time as the solvent evaporates gradually, and thus, the concentration increase due to solvent evaporation is partially counteracted.

Under low NR concentration (e.g., absorbance of longitudinal UV−vis band = 0.3), as shown in Figure 1A,B, there are domains of closely packed parallel arrangements of NRs on a homogeneous ODS-SAM substrate and some spherical particles of byproduct perturb and separate the ordered domains of NRs. That is to say, the uniformity of particles without differently shaped particles is important for ordering the assembly. Spontaneous formation of perpendicularly arranged NR assemblies was also obtained under this condition, as shown in Figure 1C,D, in which the NRs were packed into a superlattice with hexagonal geometry. However, it is regrettable that a parallel structure dominates on the substrate. Moreover, under much lower concentration, no vertical orientation of NRs was observed and most NRs deposited as a loose assembly of small parallel aggregates in a side-by-side mode on the substrate (Figure S2 in the Supporting Information).

Growth of Gold NR Superlattices at a High NR Concentration on a Homogeneous ODS-SAM Substrate. If a suspension at a higher concentration (e.g., UV−vis absorbance = 1.4) was used, many parallel stripes or lines were deposited, extending over the whole homogeneous ODS-SAM substrate, as shown in Figure 2A, where the arrow indicates the downtrend direction of the liquid interface descending due to solvent evaporation. The interval between the stripes was within the range of 100−200 μm, and the width of each stripe was ca. 10 μm. Moreover, the line intervals and NR densities on the stripes showed less variation from the top to the bottom of the substrate. After the formation of one NR stripe, the deposition process abruptly decreases and particles are scarcely observed between the stripes.

The assembly structure within each stripe was formed by aligned NR arrays with the parallel or perpendicular direction to the substrate. Compared with the assembly structure under low NR concentration (as shown in Figure 1), the perpendicular alignments obviously increased. Moreover, multilayers grown

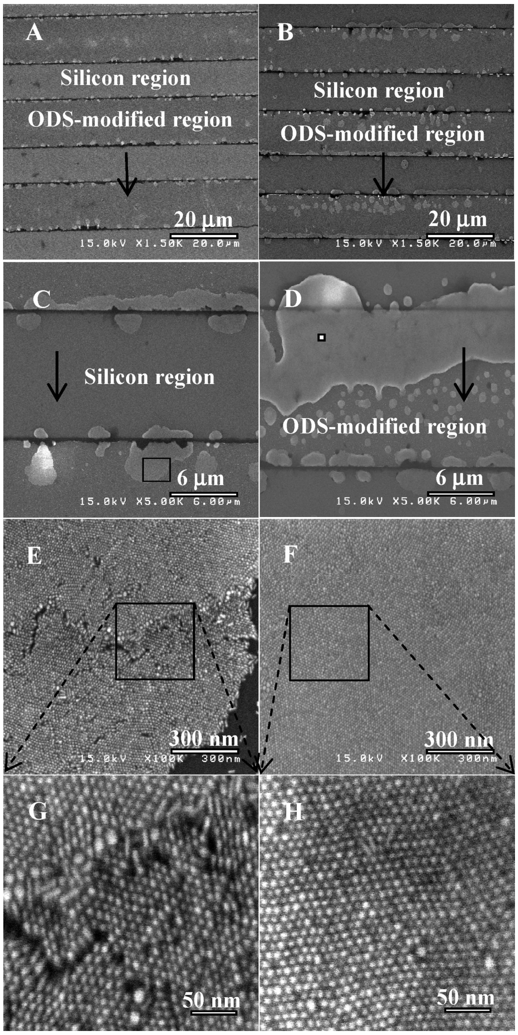

Figure 3. SEM images of NR superlattice domains on patterned substrates at different magnifications. UV−vis absorbance at longitudinal band of NR dispersion: (A,C,E,G) ∼0.3; (B,D,F,H) ∼1.4. The arrows indicate downtrend of the liquid interface.

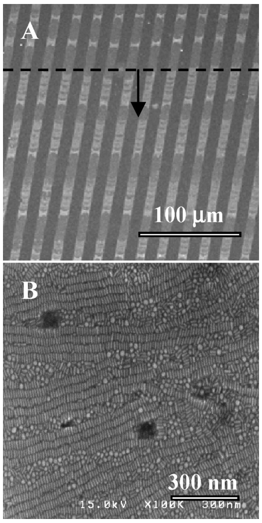

Figure 4. (A) SEM image of a spontaneous pattern of NRs when the patterned substrate with the longitudinal stripe axis was tilted at a certain angle (almost perpendicular) to the liquid interface. (B) Enlarged SEM of the bright region in (A). The arrow denotes downtrend of the liquid interface.

on the substrate showed a high degree of ordering with compactness over a wide area. It can be confirmed from the magnified image of the stripe edge in Figure 2B that the gold NRs aggregate together in multilayers with a perpendicular orientation on the substrate and in a hexagonally close-packed superlattice. The rod side is also visible at the edge of each monolayer, as seen in Figure 2C, which is the magnified image of the marked square area in Figure 2B. In addition, unfavorable spheres are deposited at the edge of the monolayer. The illustration reveals the assembly structure between neighboring layers. However, it should be noticed that the flat superlattice (monolayer) surface is not large enough.

Growth of Gold NR Domains on a Patterned Substrate. A topological pattern was obtained via photolithographic technology in which vacuum ultraviolet light at 172 nm was used to expose the PMMA photoresist. Combined with chemical modification, periodic patterns of silicon and ODS-SAM stripes were formed on the substrate. With regard to the adsorption process of NRs, it should be pointed out that the longitudinal direction of these stripes is parallel to the liquid interface.

It was found that when the NR concentration is low, as shown in the SEM image in Figure 3A, the domains of NRs appeared on both the top and bottom edges of the ODS stripe and only on the bottom edge of the silicon stripe. On the other hand, some NR domains and randomly distributed NRs were distributed on the ODS stripe surface but scarcely on the silicon stripe surface. The results indicate that the NRs prefer to adsorb on the ODS stripe surface. Moreover, the domain sizes change from submicrometers to a few micrometers.

When the NR concentration increases, a similar mode but with an obviously large amount of adsorption (or large size of domains) is observed (see Figure 3B). The domains are as large as several square millimeters. It should be noticed that the upper portion of the ODS stripe surface (with respect to the descending direction of the liquid interface) has a larger number of domains than the edges, whereas the top edge of the silicon stripe displays minor adsorption. Clearly, the stripe patterns have an effect on the assembling process of NRs.

Growth of Gold NR Superlattices on a Patterned Substrate. As for the ordered structure in NR domains consisting of a mono- or oligolayer of NRs (see Figure S3 in the Supporting Information), it can be seen from Figure 3C,E,G of the specimen from the dilute NR dispersion that almost all rods tend to align vertically on the substrate, forming domains of close-packed "standing" NRs.[9] It should also be noticed that there are many defects in the domain.

From the images of the specimen at a high NR concentration, as shown in Figure 3D,F,H, it can be seen that the surface of the domain is very flat and has fewer defects. Moreover, the regularly close-packed NRs are aligned perpendicularly to the substrate, and the ordered packing is over the whole domain. It is also important to note here that no domains of parallel superlattices are observed over the whole patterned substrate.

Only the longitudinal axis of stripes parallel to the liquid interface is supposed to undergo a cooperative relationship between topological patterns and domain growth. To confirm this supposition, the longitudinal axis of the stripe was tilted at an angle or vertical to the liquid interface. The adsorption phenomenon was similar to that of the nonpatterned substrate (Figure 2A), but some spontaneous stripes deposited only on the silicon surface region, as shown in Figure 4A, in which most NRs aggregated in a parallel stripe mode (Figure 4B). Moreover, the width of the stripes was wider, but the distance between stripes was shorter than that on the nonpatterned substrate. With these results, it is confirmed that the direction

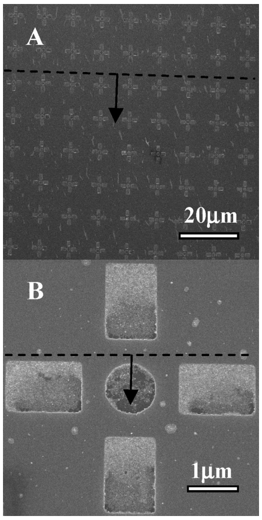

Figure 5. (A) SEM image of a pattern with different shapes and small sizes, which is vertically immersed in the NR suspension. (B) Enlarged SEM image of one set in the pattern. The arrow denotes downtrend of the liquid interface.

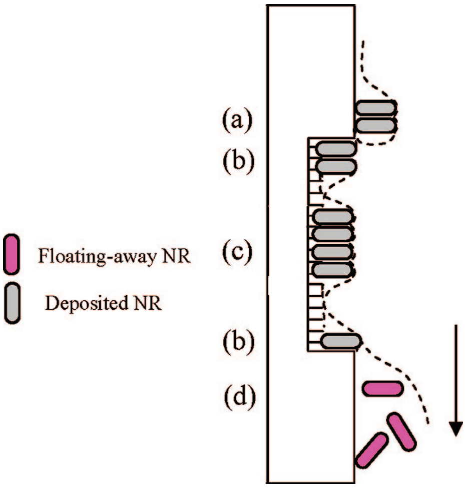

Figure 6. Gold NR confinements at the contact line in different parts (prior to, within, and over the etched pattern, listed as a, b, c, and d) on the substrate. The arrow denotes downtrend of the liquid interface.

of stripe patterns strongly influences the perpendicular assembling in NR superlattices.

In addition, instead of a striped pattern, the patterned substrate with different shapes in small scale was treated with a NR suspension of UV−vis absorbance ∼1.4. It was found that the NRs almost occupied the whole area of the ODS-modified pattern, as shown in Figure 5A, although the density gradation of NRs in each set of patterns arose as the liquid interface receded (see Figure 5B). There is no doubt that the shape of the pattern strongly influences the deposition of gold NRs.

Growth Mechanism of NR Perpendicular Superlattices. An observation to be discussed is the primitive formation of NR arrays along the edge of the stripe pattern in the evaporation process. Wolf and his co-workers[16] have found that capillary forces and convective flows could be exploited to assemble hydrophilic polystyrene nanospheres into superlattices (mono- or multilayers) on a substrate with or without a pattern. Their approach is applicable to explain the self-assembling of anisotropic gold NRs from organic suspensions in the present work since the NR assembly growth can depend on the wetting properties and topological patterning of the substrate.

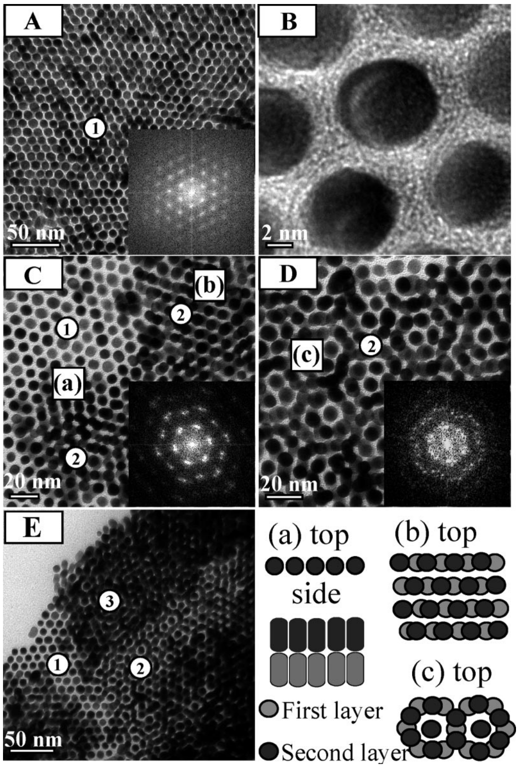

Figure 7. TEM images of the perpendicular arrangement of gold NRs: (A) monolayer, (B) high-resolution image of the monolayer, (C,D) bilayer, and (E) trilayer. Insets show corresponding FFT diffractions from superlattices. The numbers represent the number of array layers. The schemes from (a) to (c) illustrate details of the layer structure.

At the bottom edge of the silicon stripe (part a in Figure 6), the geometry (edge) effect of the patterns induces droplets of the NR suspension and, at the same time, the convective flow pulls down the NRs in the droplets toward the edge. At the top and bottom edges of the ODS stripe, the combined effects of convective flow and attractive capillary force will lead to the formation of NR domains, as seen in part b in Figure 6. When the liquid interface descends over the ODS-modified pattern, as shown in part d in Figure 6, the NR suspension cannot remain on the silicon stripe surface and, therefore, no NRs will deposit at this region due to the weak interaction of NRs with the relatively hydrophilic silicon stripe. When the concentration of the NR suspension increases, the liquid film spreads out even the hydrophobic ODS-modified stripe surface with the aid of NR/substrate interaction. Thus, some domains can be also observed in this region (see part c in Figure 6). It should be pointed out that the use of very shallow patterns does not affect the motion of NRs at the stripe edge toward the drying process.[16]

As for the superlattice growth in the droplets or liquid film, the dominant driving forces for NR alignment are attributed to the combination of the NR/substrate and NR/NR interactions. The reason for NR arrays to align perpendicular to each other in this configuration is to enable functional linkers to connect neighboring rods, thus reducing the free energy of the system. In the present case, linkers are hydrophobic alkyl chains that act as a protector/stabilizer of the NRs, which are derived in the synthesis process and raise the hydrophobic interaction force. In the dilute NR dispersion, the possibility of such interaction between NRs is less.

Interlayer Ordering in Superlattices. Although a hexagonal closest-packing monolayer structure in NR superlattices has been confirmed by TEM and small-angle X-ray scattering,[9] interlayer ordering has scarcely been discussed. To confirm the interaction between superlattice monolayers, TEM was examined at different portions of the superlattice.

As seen in Figure 7A, round (hexagonal) cross sections of NRs were hexagonally close-packed, and the fast Fourier transform electron diffraction (FFTED) (the inset in Figure 7A) shows a hexagonal superlattice. Figure 7B, under higher magnification, indicates that the space between NRs, ∼2 nm, is occupied by interdigitated protectors/stabilizers of the NRs, which surround each NR to form a hydrophobic shell. The double or triple layers of the hexagonal crystal structure were observed at different portions (see Figure 7C,D,E). FFTEDs from selected regions point out two (the inset in Figure 7C) or several (the inset in Figure 7D) sharp out-of-phase diffraction spots that reveal the rotation in the azimuthal alignment occurring at this location. The corresponding top views of the perpendicular arrangement of NRs in portions (a), (b), and (c) are schematically shown in Figure 7. It is indicated from these results that interlayer interaction in superlattices is not explicitly confirmed but has various possibilities.

Conclusions

In this paper, a patterned silicon substrate with hydrophobic stripes was successfully applied for growing gold NR superlattices. Some results clearly indicate the formation of perpendicular superlattices. Moreover, the substrate surface is one of the most important factors, and the NRs must be either positively attracted or at least not repelled by hydrophobic (ODS-SAM) surfaces. For the relatively hydrophilic silicon stripe, it is clearly more favorable for the gold NRs to stay in solvent rather than attach to the substrate surface. In addition, the stripe edge is envisaged as a new platform to control the NR self-assembling. This new strategy allows generation of crack-free colloidal crystals over several square millimeters.

Significantly, stable perpendicular NR superlattices of a large scale can be easily produced, thus leading the way to the use of perpendicular NR superlattices in numerous applications. The present result is the first step to open new applications using morphology-controlled anisotropic gold NR superlattice assemblies.

Acknowledgment. We thank Prof. Shunri Oda at the Tokyo Institute of Technology and Mr. Masahiro Morikawa and Mr. Motohiro Yamada at Konica Minolta Technology Center, Inc. for their help in photolithography and their valuable discussions. We also acknowledge Dr. Koji Mitamura at the Nagoya University for guidance in gold NR preparation. This work was carried out under the partial financial support from Konica Minolta Technology Center, Inc.

Supporting Information Available: Additional characterizations for superlattice growth by TEM, X-ray diffraction spectrum, energy-dispersive X-ray spectrum, and SEM are provided. This material is available free of charge via the Internet at http://pubs.acs.org.

References and Notes

(1) Losic, D.; Shapter, J. G.; Mitchell, J. G.; Voelcker, N. H. *Nanotechnology* **2005**, *16*, 2275–2281.

(2) Seifarth, O.; Krenek, R.; Tokarev, I.; Burkov, Y.; Sidorenko, A.; Minko, S.; Stamm, M.; Schmeisser, D. *Thin Solid Films* **2007**, *515*, 6552–6556.

(3) Ryan, K. M.; Mastroianni, A.; Stancil, K. A.; Liu, H.; Alivisatos, A. P. *Nano Lett.* **2006**, *6*, 1479–1482.

(4) Gupta, S.; Zhang, Q.; Emrick, T.; Russell, T. P. *Nano Lett.* **2006**, *6*, 2066–2069.

(5) Kim, F.; Kwan, S.; Akana, J.; Yang, P. *J. Am. Chem. Soc.* **2001**, *123*, 4360–4361.

(6) Nikoobakht, B.; Wang, Z. L.; El-Sayed, M. A. *J. Phys. Chem. B* **2000**, *104*, 8635–8640.

(7) Jana, N. R.; Gearheart, L. A.; Obare, S. O.; Johnson, C. J.; Edler, K. J.; Mann, S.; Murphy, C. J. *J. Mater. Chem.* **2002**, *12*, 2909–2912.

(8) Ahmed, S.; Ryan, K. M. *Nano Lett.* **2007**, *7*, 2480–2485.

(9) Mitamura, K.; Imae, T.; Saito, N.; Takai, O. *J. Phys. Chem. B* **2007**, *111*, 8891–8898.

(10) Zhang, C.; Zhang, X.; Zhang, X.; Fan, X.; Jie, J.; Chang, J. C.; Lee, C. S.; Zhang, W.; Lee, S. T. *Adv. Mater.* **2008**, *20*, 1716–1720.

(11) Liu, S.; Maoz, R.; Sagiv, J. *Nano Lett.* **2004**, *4*, 845–851.

(12) Kwon, S. J.; Park, J.-H.; Park, J.-G. *J. Electroceram.* **2006**, *17*, 455–459.

(13) Liu, S.; Tok, J. B. H.; Locklin, J.; Bao, Z. *Small* **2006**, *2*, 1448–1453.

(14) Liu, S.; Wang, W. M.; Mannsfeld, S. C. B.; Locklin, J.; Erk, P.; Gomez, M.; Richter, F.; Bao, Z. *Langmuir* **2007**, *23*, 7428–7432.

(15) Ling, X. Y.; Malaquin, L.; Reinhoudt, D. N.; Wolf, H.; Huskens, J. *Langmuir* **2007**, *23*, 9990–9999.

(16) Malaquin, L.; Kraus, T.; Schmid, H.; Delamarche, E.; Wolf, H. *Langmuir* **2007**, *23*, 11513–11521.

(17) Li, F.; Zhu, M.; Liu, C.; Zhou, W. L.; Wiley, J. B. *J. Am. Chem. Soc.* **2006**, *128*, 13342–13343.

(18) Fan, Z.; Ho, J. C.; Jacobson, Z. A.; Yerushalmi, R.; Alley, R. L.; Razavi, H.; Javey, A. *Nano Lett.* **2008**, *8*, 20–25.

(19) Carbone, L.; Nobile, C.; De Giorgi, M.; Sala, F. D.; Morello, G.; Pompa, P.; Hytch, M.; Snoeck, E.; Fiore, A.; Franchini, I. R.; Nadasan, M.; Silvestre, A. F.; Chiodo, L.; Kudera, S.; Cingolani, R.; Krahne, R.; Manna, L. *Nano Lett.* **2007**, *7*, 2942–2950.

(20) Sugimura, H.; Hozumi, A.; Kameyamaand, T.; Takai, O. *Surf. Interface Anal.* **2002**, *34*, 550–554.

(21) Yamazaki, T.; Imae, T.; Sugimura, H.; Saito, N.; Hayashi, K.; Takai, O. *J. Nanosci. Nanotechnol.* **2005**, *5*, 1792–1800.

JP808864V